

# Alternative Splicing in Pancreatic Ductal Adenocarcinoma Leads to Dysregulated Immune System

Fatimah A. Abdul Jabbar<sup>1</sup>, Rawaa AlChalabi<sup>1</sup>, Ahmed Yaseen AL-Tarboolee<sup>1</sup>, Sema A. Shaban<sup>\*2</sup>, Ahmed AbdulJabbar Suleiman<sup>3</sup>

<sup>1</sup>College of Biotechnology, AL-Nahrain University, Jadiriya, Baghdad, Iraq

<sup>2</sup>College of Sciences, Tikrit University, Tikrit, Iraq

<sup>3</sup>College of Science, University of Anbar, Ramadi, Anbar, Iraq

**Abstract.** Pancreatic ductal adenocarcinoma (PDAC) is a highly lethal malignancy that poses a significant global health threat, marked by a substantial increase in prevalence and mortality rates. Accounting for 90 % of pancreatic cancer cases, PDAC carries a dismal prognosis, and current therapeutic approaches, including immunotherapy, face challenges due to poor immunogenicity. This study aimed to discover differentially expressed immune genes shared between PDAC and normal samples from two datasets obtained from the NCBI GEO Dataset. The RNA-seq pipeline was employed for gene expression analysis, and enrichR facilitated functional enrichment analysis of biologically and statistically significant genes. Predictions of immune infiltration cells and corresponding genes, along with their immune responses, were made using the ScType database and the immunedeconv package, respectively. Verification of gene expression levels was conducted through GEPIA2, Expression Atlas, and literature review. Additionally, isoform-switching analysis of dysregulated genes aimed to uncover alternatively spliced pathogenic isoforms in PDAC. Notably, four immune genes (EPHA2 upregulated, GNG11, CRHBP, and FCER1A downregulated) were found to be common in both datasets and were highly implicated in PDAC. The dysregulated immune genes influenced molecular functions, including protein binding, transmembrane receptor protein tyrosine kinase activity, protein tyrosine kinase activity, and cadherin binding for upregulated genes. Downregulated genes were associated with GTPase activity and ribonucleoside triphosphate phosphatase activity. This study suggests these immune genes as potential prognostic biomarkers for effective PDAC treatment. However, further investigations are essential to unravel the functional perspectives of potential isoforms.

**Key words:** PDAC, alternative-spliced genes in PDAC, immune-infiltrating genes in PDAC, PDAC dysregulated immune genes, PDAC immune therapeutic biomarkers.

## INTRODUCTION

One lethal malignancy is pancreatic cancer characterized by the development and growth of cancer cells within the pancreatic tissues [1]. Classified as the seventh most common cancer-related mortality globally, it presents challenges due to poor survival rates and difficulties in early diagnosis [1, 2]. According to pancreatic cancer data from GLOBOCAN 2020, there were 495,773 new cases reported, with 466,003 recorded deaths across both sexes. The age-standardized incidence rate of pancreatic cancer is 5.7 in men and 4.1 in women per 100,000 persons, underscoring its higher prevalence in men worldwide. Additionally, Asia has witnessed the highest incidence (47.1 %), mortality (48.1 %), and 5-year prevalence (47.4 %) rates [3].

Pancreatic malignancies are categorized into benign and malignant neoplasms. Benign neoplasms encompass serous cystadenoma, intraductal tubulopapillary neoplasm, intraductal

---

\*sema.alsham@tu.edu.iq

papillary mucinous neoplasms, and mucinous cystic neoplasms [4]. Conversely, malignant neoplasms are further classified into those of ductal origin and non-ductal origin [5].

Among all pancreatic malignancies, pancreatic ductal adenocarcinoma (PDAC) in the exocrine pancreas stands out as the most common and aggressive form of pancreatic cancer [6]. PDAC constitutes a staggering 90 % of overall pancreatic cancer cases and is associated with a poor prognosis [7, 8]. Predominantly occurring in the head of the pancreas, PDAC often involves the duodenum or ampulla, presenting challenges in pinpointing its exact origin [9].

Numerous well-established studies have identified PDAC as being frequently associated with a mutation in the oncogene KRAS, marking it as the most common genetic cause. Other commonly mutated genes include the tumor suppressors SMAD4, CDKN2A, and TP53 [10, 11]. Despite its asymptomatic nature in its early stages, PDAC progresses rapidly, and non-specific symptoms such as jaundice, nausea, fatigue, weight loss, and abdominal and back pain become evident [12, 13]. The manifestation of perineural and vascular channel invasion in PDAC contributes to its extensive spread, underscoring its inherently aggressive nature [9]. Furthermore, the lack of immune activation and low immunogenicity are linked to the aggressive behavior of PDAC [14].

Recent cancer immunotherapy, considered an effective therapeutic approach, has faced challenges in achieving success against PDAC due to its poor immunogenicity, immunological tolerance, and the presence of an immunosuppressive microenvironment [15, 16]. Within the tumor microenvironment of PDAC, macrophages and immature myeloid cells have been identified as cells that promote tumor growth. Additionally, the interaction between pancreatic cancer cells and stromal cells has been linked to various malignant characteristics of PDAC, including proliferation [17]. The intricate interactions between immune and tumor cells in this disease, crucial for understanding cancer progression and evasion, remain not clearly understood [18].

Alternative splicing, a post-transcriptional mRNA processing mechanism, can generate multiple mRNA transcripts, resulting in structurally and functionally modified proteins from a single gene. This variability in splicing can lead to malignant phenotypes, and the isoforms produced may have functional relationships or differ significantly [19, 20]. In PDAC, alternative splicing has been associated with promoting tumor progression and resistance to therapy. Notably, isoforms of CD44, a cell-surface glycoprotein, have been implicated in cancer metastasis [21]. Additionally, an isoform of the RON tyrosine kinase receptor has been identified in pancreatic cancer cell lines [22]. The significant association of alternative splicing events with the tumor immune microenvironment has been reported, impacting immune cell infiltrations [17].

Nevertheless, the identification of differentially expressed immune genes and the analysis of immune responses affected in PDAC can provide crucial insights into the mechanisms involved in the isoform switching of immune-related genes through alternative splicing of mRNAs. This process plays a pivotal role in tumor proliferation and progression, potentially resulting in the discovery of novel therapeutic biomarkers for PDAC. Furthermore, differentially expressed immune genes may also serve as therapeutic biomarkers, shedding light on the still controversial interactions between tumors and immune cells, and offering avenues to overcome the poor immune responses associated with the inherent immunogenicity challenges of PDAC.

Considering the poor immunogenicity, the lack of significantly activated immune systems, and the adverse effects of alternate splicing on immune cell infiltration, it is imperative to explore the alternate splicing events of immune-related genes. This study is designed to utilize RNA sequencing data from PDAC patients and corresponding normal individuals to analyze the dysregulated immune response generated against PDAC. The identification of differentially expressed genes is followed by the filtration of immune-related genes. Subsequently, the investigation extends to the isoforms of immune-related genes generated due to PDAC. Consequently, this study aims to pinpoint dysregulated immune response-related biomarkers in PDAC that can serve as new therapeutic targets for further studies.

## METHODOLOGY

### Study overview

The present study aimed to identify dysregulated immune system genes, with a focus on understanding how alternative splicing of these genes may contribute to poor immune response in PDAC patients. To achieve this objective, a multi-step approach was employed. Firstly, the RNA-seq pipeline was utilized to analyze two datasets consisting of tumors and their adjacent normal tissue samples from pancreatic cancer patients. Subsequently, immune system-associated genes were extracted from the pool of common dysregulated genes identified in both datasets, highlighting genes with shared dysregulation in the immune system. The expression levels of these common dysregulated genes were then validated through GEPIA, Expression Atlas, and a review of the literature.

Furthermore, functional enrichment analysis was conducted on the identified common genes to gain insights into the biological processes, molecular functions, cellular components, and pathways associated with these dysregulated immune genes. Lastly, isoform switching analysis was performed specifically on the common upregulated and downregulated immune genes to elucidate their biological relevance to PDAC. The study design is illustrated in Figure 1.

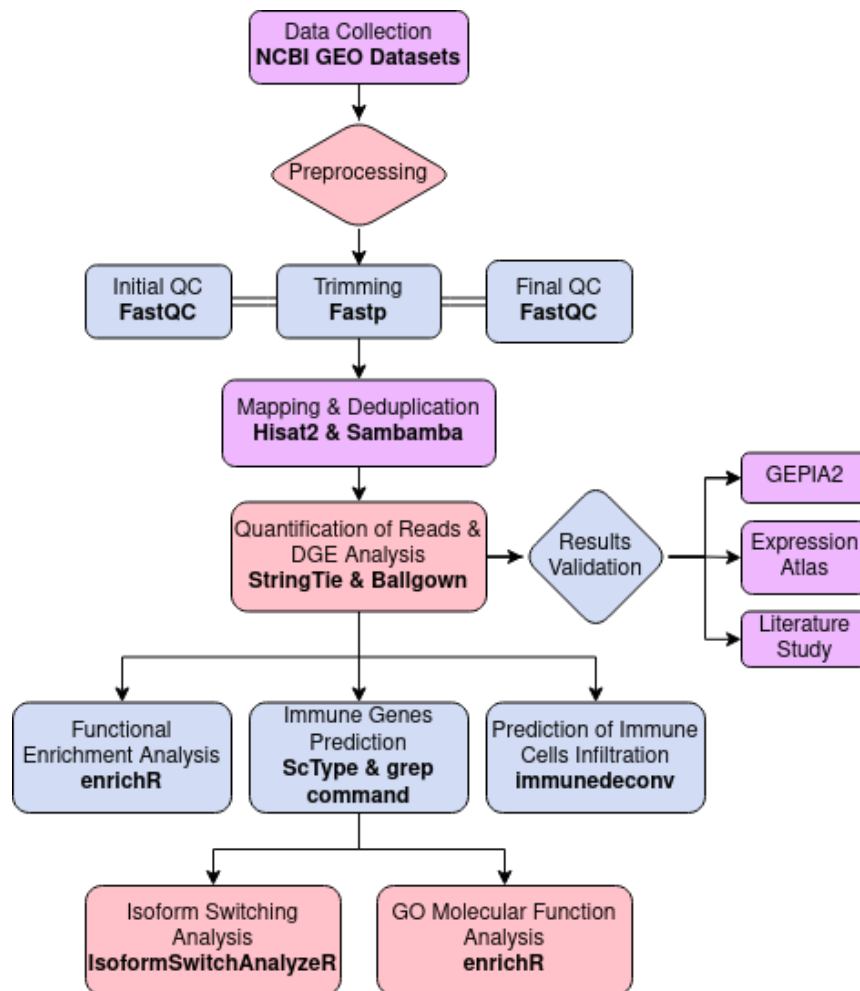


**Fig. 1.** Overall workflow of PDAC study.

### Collection of data

The RNA-seq datasets were obtained from the Gene Expression Omnibus (GEO) with the following accession numbers: GSE171485 and GSE119794 [23]. GEO serves as an international public repository for microarray, high-throughput sequencing, and next-generation sequence

functional genomics datasets and is supported by the National Center for Biotechnology Information (NCBI) [24]. Specifically, the GSE171485 dataset comprised 6 samples from PDAC patients and 6 samples from normal individuals. On the other hand, the GSE119794 dataset included (9 samples from pancreatic cancer patients, consisting of 5 tumor samples and 4 normal samples). Both datasets were sequenced using the Illumina HiSeq 2000 platform.

### ***RNA-seq preprocessing, mapping, and post-processing***

Raw reads obtained from the sequencer often contain contaminants such as poor-quality reads, adapters, and primer contents. To address this issue, raw reads underwent preprocessing before alignment. The FastQC tool was utilized to assess the quality of raw reads, considering parameters such as per-base sequence quality, GC content, per-base N content, sequence length distribution, sequence duplication levels, overrepresented sequences, and adapter content [25]. Poor-quality reads were then trimmed using the FastP tool, with parameters like *-i* for raw FASTQ sample, *-o* for output, and *-w* for multi-core processing. This step aimed to eliminate PCR artifacts and low-quality reads, ensuring the generation of high-quality data for downstream analysis [26].

Following trimming, the quality of the cleaned reads underwent reassessment using the FastQC tool. Subsequently, the cleaned reads were aligned against the reference human genome (GRCh38) using the Hisat2 aligner. To avoid false estimation of gene expression, duplicates, also known as PCR artifacts, were identified and removed from mapped reads using a Sambamba command-line module named markdup, with the *-r* flag employed in the process [27].

### ***Read quantification and DEA analysis***

Abundances of gene expression were estimated using the StringTie tool [28]. StringTie performed a three-step process to generate count reads: initially, it assembled alignments into partial and full-length transcripts, creating multiple isoforms containing millions of short read sequences. Subsequently, transcripts were merged to establish a consistent set across all samples, and gene quantification was carried out using the merged transcripts as a reference. The *-eB* option was employed to generate expression counts in the Ballgown table format.

Differentially expressed genes (DEGs) between pancreatic cancer patients and normal individuals were analyzed using the Ballgown 2.30.0 package in R 4.2.2. Biologically and statistically significant genes between PDAC and normal samples were identified based on reads per kilobase of exon per million reads mapped (FPKM) normalized expression, analyzed by Ballgown using logFC values and p-values, respectively. A threshold of P-value < 0.05 and |LogFC| > 1 was applied to define upregulated and downregulated genes. Additionally, significant DEGs were visually represented through a Volcano plot.

### ***Identification of common dysregulated genes***

Common significant dysregulated genes between the two datasets were identified using Venny 2.1.0 (<https://bioinfogp.cnb.csic.es/tools/venny/>) and the number of common upregulated and downregulated genes were illustrated as Venn diagrams.

### ***Validation of common dysregulated genes***

The dysregulated expression of significant upregulated and downregulated genes common between the two datasets was further validated through Gene Expression Profiling Interactive Analysis (GEPIA2), Expression Atlas, and a literature review [29, 30]. GEPIA2 serves as a valuable resource for gene expression analysis, leveraging tumor and normal samples from The Cancer Genome Atlas (TCGA) and Genotype-Tissue Expression (GTEx) databases. The Expression Atlas database, supported by the European Bioinformatics Institute (EBI), provides insights into gene expression patterns using data from RNA-seq and microarray studies, as well as protein expression from proteomics studies.

**Functional enrichment analysis**

Functional enrichment analysis, encompassing GO term analysis and KEGG pathway analysis of the common dysregulated genes, was conducted using the enrichR 3.1 package in R 4.2.2 [31]. Upregulated and downregulated genes were analyzed separately. The plotEnrich() function was employed to generate bar plots depicting GO terms (biological process, molecular function, and cellular component) and KEGG pathways. Notably, enrichment terms were sorted based on the least p-value.

**Prediction of immune-system-related marker genes**

Immune marker genes were identified by comparing against the ScType gene marker database [32]. ScType is a fully automated database that relies on cell type identification of single-cell RNA-seq profiles, utilizing a comprehensive cell marker database based on experimentally validated expression signatures as background information. Hence, the Cell Marker Database of ScType was utilized to filter out immune system-related genes. Subsequently, GO molecular function (MF) analysis of the shortlisted dysregulated immune genes was conducted using GeneCodis 4 [33].

**Isoform switching analysis**

Transcript-level expression profiles between PDAC and normal individuals were identified through isoform switching analysis using the IsoformSwitchAnalyzeR package (v1.16.0) in R 4.2.2 [34]. Quantification files and merged annotations obtained through StringTie were inputted into IsoformSwitchAnalyzeR, along with transcript files and a design file containing sample IDs and their corresponding conditions. The IsoformSwitchTestDEXSeq() function was applied to predict Differential Isoform Usage (DIU) based on a differential isoform (dIF) cutoff of 0.1 and a gene ExpressionCutoff of 0.5, providing relative abundances of all isoforms of a gene between PDAC and normal samples.

The longest Open Reading Frames (ORFs) were shortlisted using the analyzeORF function with the longest orfMethod. Subsequently, shortlisted ORF sequences were extracted through extractSequence, generating two files containing nucleotide and protein sequences. Functional consequences for ORFs, including coding potential, signal peptides, protein domains, and intrinsically disordered regions (IDRs), were identified through CPC2, SignalP, Pfam, and IUPred3, respectively. Functions such as analyzeCPC2, analyzeSignalP, analyzePFAM, and analyzeIUPred2A were utilized to assign functional consequences to the transcripts. Finally, the switchPlot function was employed to plot dysregulated immune gene isoforms in PDAC [35].

**Prediction of immune response in PDAC**

Immune cell infiltration and immune response are identified in the tumor microenvironment to bring about effective treatment against cancer [36]. To elucidate the immune response, a deconvolution method was employed using the deconvolute function of the immunedeconv 2.1.0 package in R 4.2.2 [37]. Two deconvolution methods majorly, quanTIseq and MCPcounter, were utilized to get the immune cell type fraction in the form of scores for all the samples and to compare scores between samples across each cell type individually, respectively [35, 38].

**RESULTS****Identification of dysregulated genes**

Expression profiling of 12 pancreatic samples ( $n = 6$  tumor;  $n = 6$  normal) under accession ID: GSE171485 revealed a total of 484 dysregulated genes (both upregulated and downregulated) in PDAC patients. Among these, 351 genes were overexpressed with a fold change value  $> 1$  and a  $P$ -value  $< 0.05$ , while 133 genes were underexpressed, exhibiting an FC value  $< -1$  and  $P$ -value  $< 0.05$  in PDAC. The biologically and statistically significant dysregulated genes are illustrated in Figure 2. Additionally, the top 10 upregulated and

downregulated genes, with respect to logFC values, are presented in Table 1 and Table 2, respectively. The top 10 significant upregulated genes included MSLN, MUCL3, TFF1, COL17A1, GJB3, KLK7, TRIM29, FAM83A, FAM25BP, and S100A14, whereas the top 10 downregulated genes comprised RPL21P7, RERGL, RPL19P16, VIT, NUDT7, CCN5, ATP1A2, CNTFR, DPT, and IQCH-AS1.

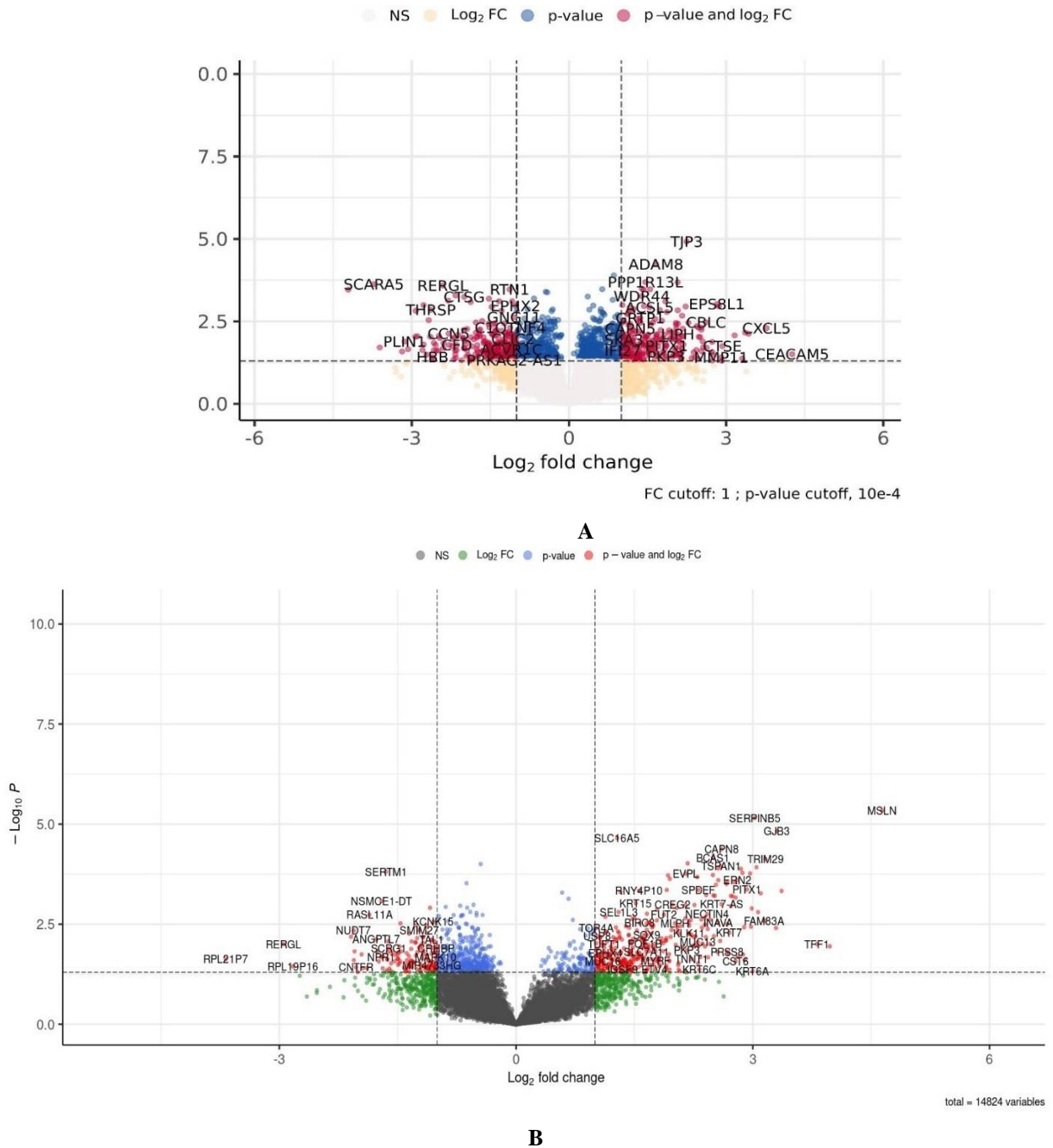


**Fig. 2.** Volcano plots from RNA-seq analysis depict differentially expressed genes in two PDAC datasets: **(A)** Enhanced Volcano plot illustrates differentially expressed genes in PDAC dataset GSE119794. Biologically significant genes are positioned on the x-axis based on Log2FC (cutoff: +1), while the y-axis represents statistically significant genes in terms of Log10P value (cutoff < 0.05). Upregulated and downregulated genes are highlighted in red dots. **(B)** Enhanced Volcano plot portrays differentially expressed genes in PDAC dataset GSE171485. Biologically significant genes are displayed on the x-axis according to Log2FC (cutoff: +1), while the y-axis denotes statistically significant genes based on Log10P value (cutoff < 0.05). Upregulated and downregulated genes are indicated by red dots.

Furthermore, transcriptomic data analysis of GSE119794, consisting of 10 samples (5 tumors vs. 4 adjacent normals), revealed 517 significantly dysregulated genes. Among these, 249 genes were upregulated, and 268 genes were identified as down-regulating genes, exhibiting a P-value  $< 0.05$  and an FC value  $> 1$  and  $< -1$ , respectively. The top 10 significantly upregulated genes included CEACAM5, CXCL5, SFTA2, LGALS4, CXCL17, MSLN, CTSE, KRT16, MMP11, and PPP1R14D. Conversely, PI16, SCARA5, IAPP, ADIPOQ, PLIN1, CHRDL1, IGF2, PLIN4, NGFR, and SCGN were identified as the top 10 downregulated genes. Based on logFC values, the top 10 upregulated and downregulated genes are provided in Tables 3 and 4, respectively.

**Table 1.** Top 10 upregulated genes in GSE171485 PDAC dataset

Genes	P-value	logFC
MSLN	4.55E-06	4.636672538
MUCL3	0.01132635057	3.976494007
TFF1	0.009963133761	3.813063842
COL17A1	0.0004668704807	3.364852262
GJB3	1.51E-05	3.303960298
KLK7	0.003939324055	3.294303935
TRIM29	7.49E-05	3.161054181
FAM83A	0.002588314191	3.143589797
FAM25BP	0.0005366872457	3.100267093
S100A14	0.001584255445	3.066562691

**Table 2.** Top 10 downregulated genes in GSE171485 PDAC dataset

Genes	P-value	logFC
RPL21P7	0.02315281016	-3.679508156
RERGL	0.01005568213	-2.945557326
RPL19P16	0.03573510581	-2.826809393
VIT	0.00652578366	-2.090649145
NUDT7	0.004555453509	-2.057172134
CCN5	0.02510264813	-2.056499259
ATP1A2	0.01517218736	-2.046368623
CNTFR	0.03767746566	-2.02774496
DPT	0.04936993338	-2.007077992
IQCH-AS1	0.01795491618	-1.957618248

**Table 3.** Top 10 upregulated genes in GSE119794 PDAC dataset

Gene	P-value	logFC
CEACAM5	0.03	4.26
CXCL5	0.01	3.77
SFTA2	0.01	3.43
LGALS4	0.01	3.36
CXCL17	0.04	3.31
MSLN	0.01	3.16
CTSE	0.02	2.93
KRT16	0.05	2.92
MMP11	0.04	2.9
PPP1R14D	0	2.86

**Table 4.** Top 10 downregulated genes in GSE119794 PDAC dataset

Gene	P-value	logFC
PI16	0	-4.21
SCARA5	0	-3.72
IAPP	0.02	-3.61
ADIPOQ	0.03	-3.18
PLIN1	0.01	-3.14
CHRD1	0.02	-3.07
IGF2	0.01	-2.93
PLIN4	0	-2.92
NGFR	0.01	-2.89
SCGN	0.02	-2.8

***Identification of common genes among the datasets***

Using Venn 2.1.0, common upregulated and downregulated genes between the two datasets were identified. Among the upregulated genes, 94 were found to be commonly present in both datasets, while 28 common downregulated genes were identified. Venn diagrams illustrating the common upregulated and downregulated genes between the two datasets are presented in Figure 3,A and 3,B, respectively.

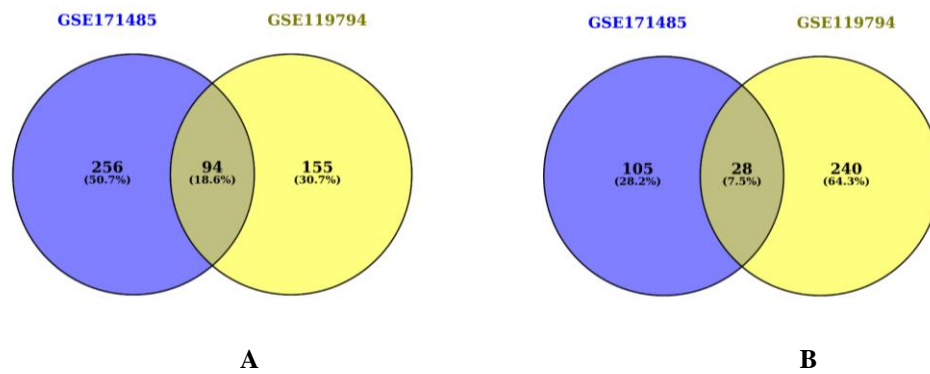


**Fig. 3:** Venn diagrams showing the number of common dysregulated genes: (A) – common upregulated genes, (B) – common downregulated genes.

### ***Validation of expression levels of common immune genes using GEPIA and ExpressionATLAS***

The expression levels of genes that were identified as common between both datasets (GSE171485 and GSE119794) were validated through GEPIA, Expression Atlas, and literature review. However, the expression data for common upregulated genes, MUCL3 and INAVA, was not available on GEPIA, and therefore, their validation was conducted using Expression Atlas. Additionally, the expression data for two upregulated genes, PLPP2 and PKD1-AS1, were not found in either of the databases, so their expressions were further verified through a literature review.

### ***GO and pathway enrichment of common genes***

The GO terms analysis associated with the dysregulated common genes among both datasets (GSE171485 and GSE119794) was conducted using enrichR. Biological processes (BP), molecular functions (MF), and cellular components (CC) GO terms were elucidated for the dysregulated genes. The upregulated genes in the datasets were found to be enriched in BP, such as epidermis development, skin development, keratinocyte differentiation, establishment of skin barrier, skin epidermis development, cell morphogenesis involved in differentiation, epidermal cell differentiation, epithelial cell morphogenesis, epithelial cell development, and tight junction assembly (Supplementary Material, Figure S1). On the other hand, the downregulated genes showed dysregulated BP, such as neuron projection extension, heart development, blood vessel morphogenesis, sulfur compound biosynthetic process, regulation of renal sodium excretion, regulation of ventricular cardiac muscle cell membrane depolarization, positive regulation of urine volume, AV node cell to bundle of His cell communication, synaptic transmission, and gap junction assembly (Figure S2).

Moreover, the dysregulated molecular functions (MF) associated with the upregulated genes included cadherin binding, actin binding, phosphatidylinositol 3-kinase regulatory subunit binding, serine-type peptidase activity, myosin V binding, myosin binding, cadherin binding involved in cell-cell adhesion, protein tyrosine kinase activity, transmembrane receptor protein kinase activity, and cell-cell adhesion mediator activity (Figure S3). However, the downregulated genes were involved in the dysregulation of MF, such as iron ion binding, gap junction channel activity involved in cell communication by electrical coupling, gap junction hemi-channel activity, neurotrophin binding, RAGE receptor binding, death receptor activity, DNA nuclease activity, transition metal ion binding, gap junction channel activity, oxidoreductase activity; acting on single donors with incorporation of molecular oxygen; incorporation of two atoms of oxygen (Figure S4).

Nonetheless, the cellular component (CC) analysis showed that the upregulated genes were mainly localized in tight junction, cell-cell junction, bicellular tight junction, cornified envelope,

apical junction complex, Golgi lumen, cortical actin cytoskeleton, platelet dense granule membrane, microvillus, and adherens junction (Figure S5). While the downregulated genes were mainly located in the Golgi lumen, collagen-containing extracellular matrix, secondary lysosome, dense core granule, connexin complex, gap junction, myofibril, intercalated disc, Golgi stack, polymeric cytoskeletal fiber (Figure S6).

**KEGG pathway analysis of common dysregulated genes from bulk RNA-seq**

The KEGG pathway analysis was performed using enrichR to indicate the dysregulated pathways due to the activity of the dysregulated genes. It revealed that the upregulated genes dysregulated pathways such as ECM-receptor interaction, tight junction, galactose metabolism, small cell lung cancer, fructose and mannose metabolism, neomycin; kanamycin and gentamicin biosynthesis, glycerolipid metabolism, central carbon metabolism in cancer, arrhythmogenic right ventricular cardiomyopathy, and insulin secretion (Figure 4). However, the pathways affected by the downregulated genes were found to be vitamin B6 metabolism, taurine and hypotaurine metabolism, ras signaling pathway, asthma, nicotinate and nicotinamide metabolism, tyrosine metabolism, tryptophan metabolism, valine; leucine and isoleucine degradation, cysteine and methionine metabolism, and regulation of lipolysis in adipocytes (Figure 5).

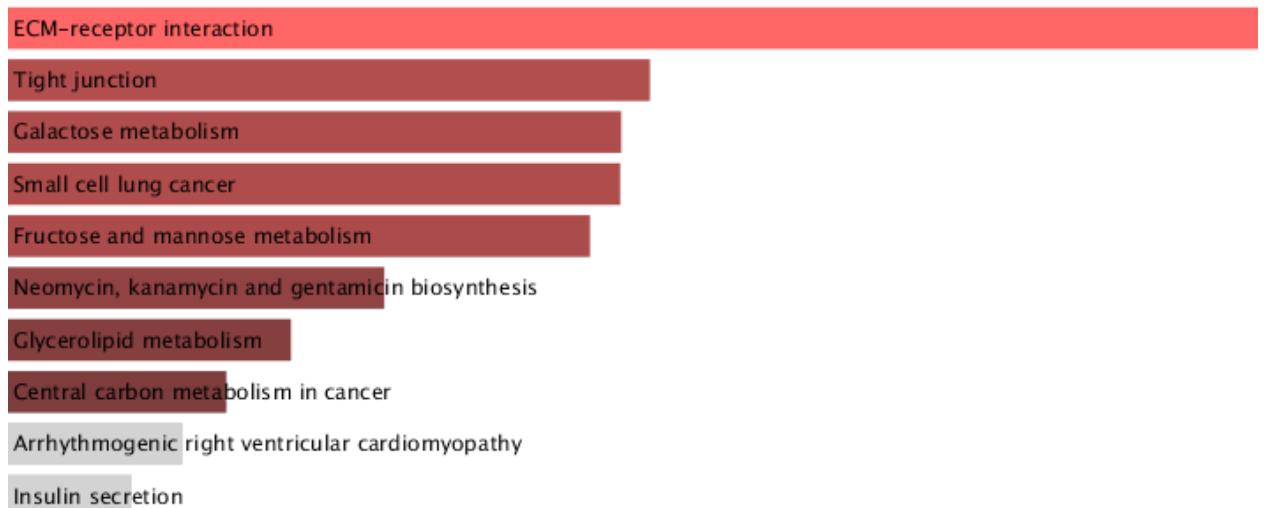


**Fig. 4.** The bar chart plot of the top 10 upregulated KEGG pathways from the KEGG pathway analysis of cancer upregulated genes, using enrichR. The red color indicates more significant pathways.

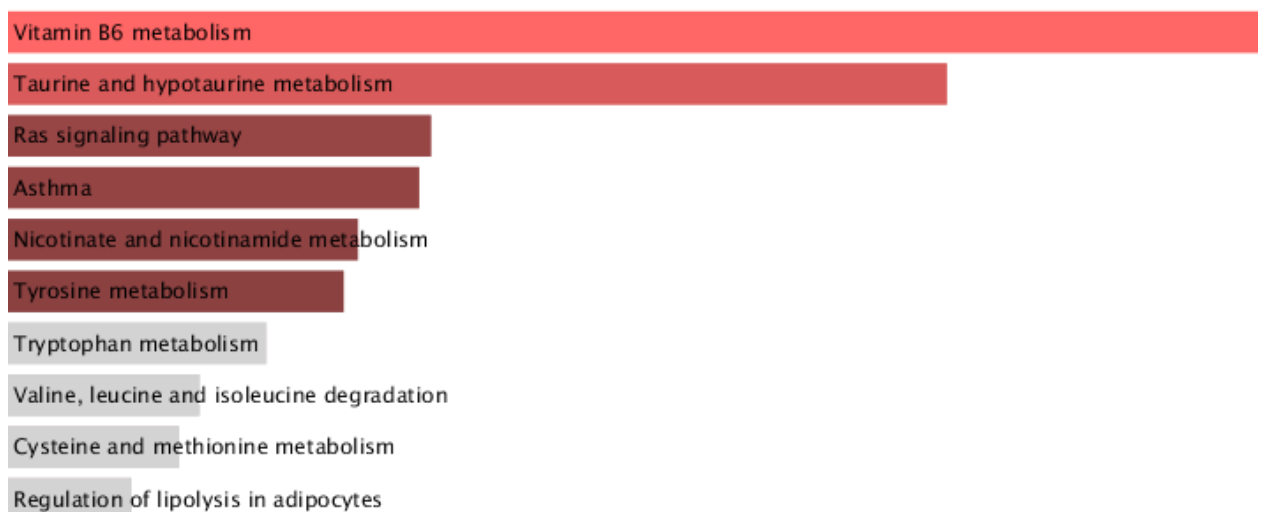


**Fig. 5.** The bar chart plot of the top 10 downregulated KEGG pathways from the KEGG pathway analysis of cancer downregulated genes, using enrichR. The red color indicates more significant pathways.

**Filtration of immune system genes**

The scType cell marker database was used to identify the genes that are involved in immune functions and involved in the regulation of the signaling pathways that play a role in the immune response against tumors. The common genes between the DEGs set and scType database were selected to identify the isoform switching in these immune system-related genes Table 5. The gene names and their functions, along with their fold change values, are represented in Table 6.

**Table 5.** Immune system-related dysregulated genes

Expression	Number of genes
Upregulated immune genes	1
Downregulated immune genes	3

**Table 6.** Shortlisted dysregulated genes involved in the immune system (P-value < 0.05) of GSE171485 and GSE119794 datasets, respectively

Gene name	P-value (GSE171485 and GSE119794 datasets)	LogFC (GSE171485 and GSE119794 datasets)	Function	Expression
CRHBP	0.7238909524	-1.010094809	Corticotropin-releasing hormone	DOWN
	0.342912567279502	-1.19		
FCER1A	0.8250759999	-1.582917688	IgE receptor that initiates allergic response	DOWN
	0.300850725284966	-2.68		
GNG11	0.6132936433	-1.181174619	Encodes lipid-anchored, cell membrane protein (involved in transmembrane signaling)	DOWN
	0.300850725284966	-1.05		
EPHA2	0.6699704272	1.608122649	Receptor tyrosine kinase responsible for bidirectional signaling into neighbouring cells	UP
	0.359087028560798	1.3		

**Isoform switching analysis and GO MF analysis of upregulated genes**

Isoform switching analysis of immune system-related genes revealed significant isoform usage for both upregulated (EPHA2) and downregulated (GNG11, CRHBP, and FCER1A) genes. For the upregulated gene EPHA2, it was observed that EPHA2 encodes two non-coding isoforms. Among them, one isoform (ENST00000358432) showed increased expression in normal, while one novel isoform (MSTRG.377.2) exhibited increased usage in cancer (Figure 6,a). Additionally, GO analysis of the upregulated immune gene identified dysregulated molecular functions (MF), including transmembrane receptor protein kinase activity, transmembrane receptor protein tyrosine kinase activity, protein tyrosine kinase activity, and cadherin binding (Figure 6,b).

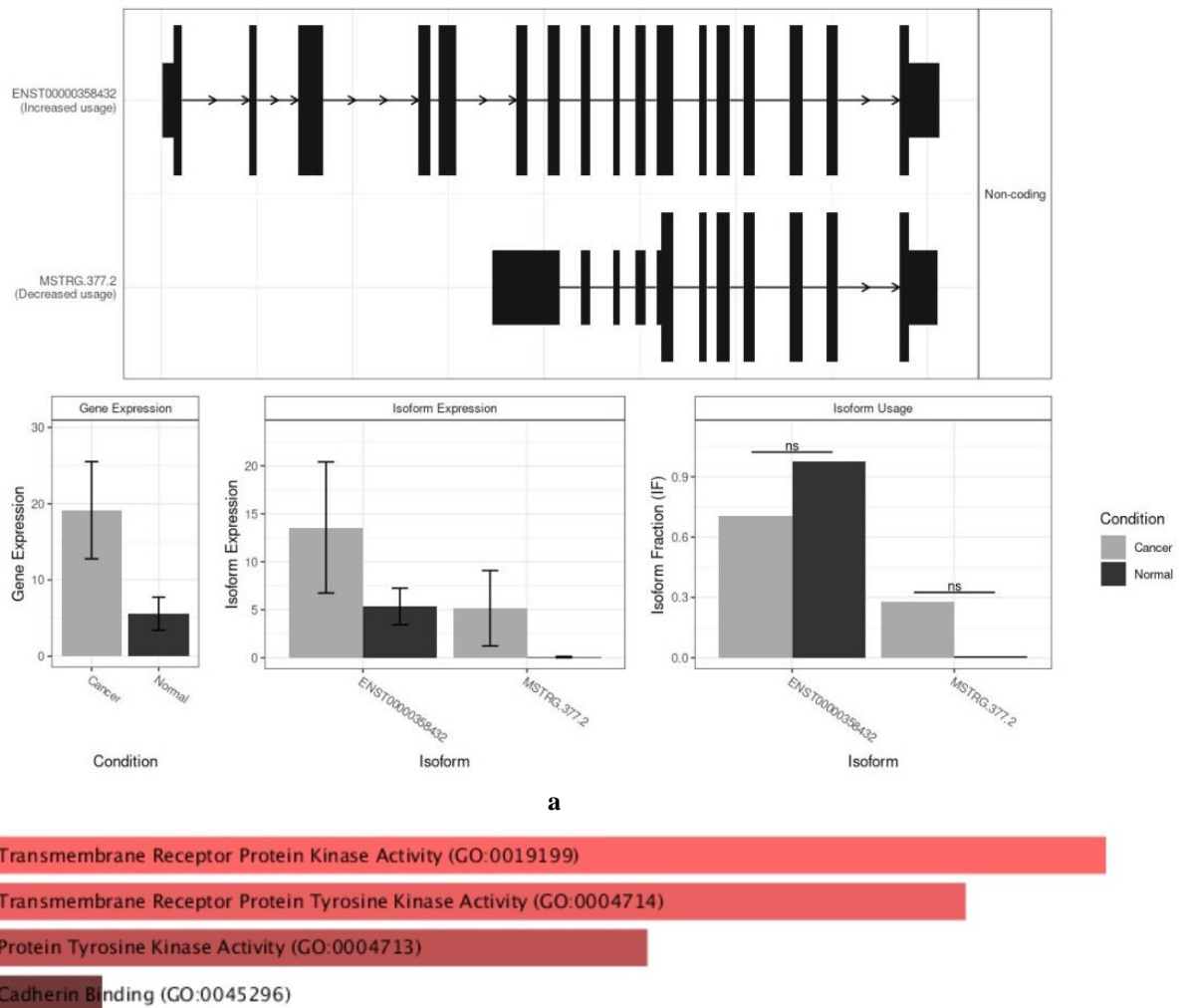


**Fig. 6.** Isoform switching analysis showing the genes and isoforms expressions, number of isoforms and isoforms usage in cancer and normal cells. It also shows the GO MF analysis of upregulated immune genes. Isoform usage of EPHA2 is shown in (a) whereas (b) shows the GO MF analysis.

*Isoform switching analysis and GO MF analysis of downregulated genes*

The isoform switching analysis of the downregulated immune system-related genes indicated that CRHBP contains a single isoform (ENST00000274368) with equal usage in cancer and normal (Figure 7,a). It was determined that FCER1A contains 2 isoforms with increased usage of only one non-coding isoform (ENST00000693622) in cancer (Figure 7,b). For gene GNG11, a single non-coding isoform (ENST00000248564) was observed with equal usage in normal and cancer-affected individuals (Figure 7,c). In addition, GO MF analysis revealed that down-regulated immune genes were primarily enriched in GTPase activity and ribonucleoside triphosphate phosphatase activity (Figure 7,d).

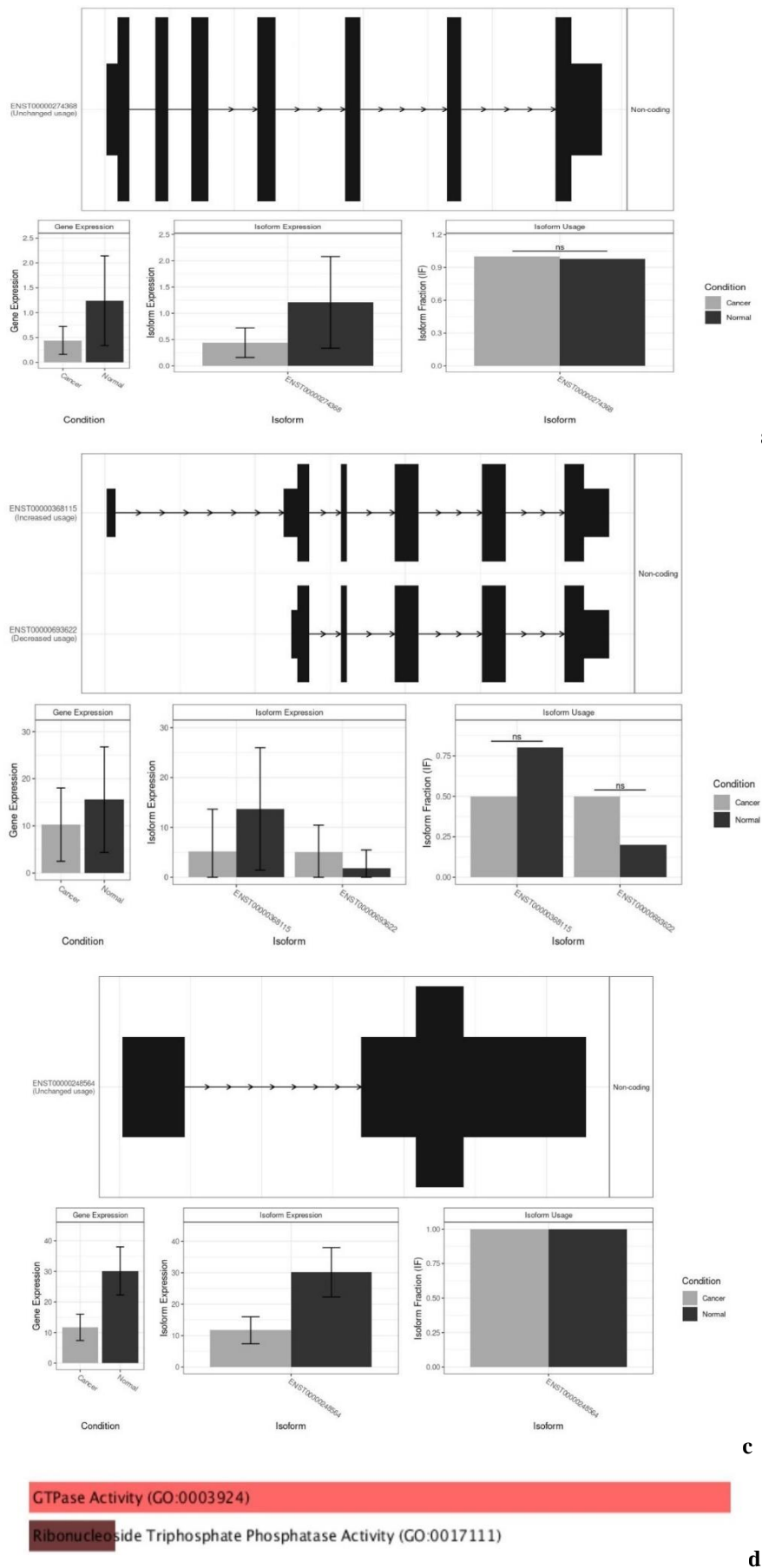


**Fig. 7.** Isoform switching analysis showing the genes and isoforms expressions, number of isoforms and isoforms usage in cancer and normal cells. It also shows the GO MF analysis of downregulated immune genes. Isoform usage of CRHBP is shown in (a), FCER1A in (b) and GNG11 is represented in (c). GO MF analysis is shown in (d).

**Immunedeconv analysis of pancreatic cancer**

The immune cell contents in PDAC and normal samples were estimated through deconvolutional approaches, primarily quanTIseq and MCPcounter methods. Figure 8, utilizing the quanTIseq method, illustrates that cancer samples exhibit a high level of B cells, Macrophages M1/M2, and Natural Killer (NK) cells. The highest level of Macrophage M1 is observed in SRR15539284 (cancer), while NK cells dominate in SRR15539282 (cancer). CD8+ T-cells are present in all the cancer samples except SRR14144012, with their highest abundance observed in SRR15539282 (cancer) and SRR15539283 (cancer). T cell regulatory (Tregs) are significantly present in all cancer samples except for SRR15539284 (cancer), with the highest level shown in SRR14144012 (cancer). Samples SRR15539281 (normal) and SRR14144011 (normal) contain the largest content of uncharacterized cells (showing no signatures) and the least amount of Macrophage M2, T cell CD8+, and NK cells.

Through the MCPcounter method (Figure 9), cancer-associated fibroblasts, cytotoxicity scores, T-cells, endothelial cells, macrophage/monocyte, myeloid dendritic cells, and neutrophils are observed in considerably high levels in 5 out of the 6 total cancer samples, including SRR14144012, SRR14144014, SRR15539284, SRR15539283, and SRR15539282. CD8+ T-cells are present in very low amounts in SRR14144012 (cancer) and in the largest amount in SRR15539282, which is consistent with quanTIseq results. The highest levels of cytotoxicity scores, myeloid dendritic cells, T-cells, and CD8+ T-cells are observed in SRR15539282 (cancer), whereas elevated levels of cancer-associated fibroblasts are found in SRR15539283 (cancer). B cells also show high levels among all cancer samples except SRR14144013.

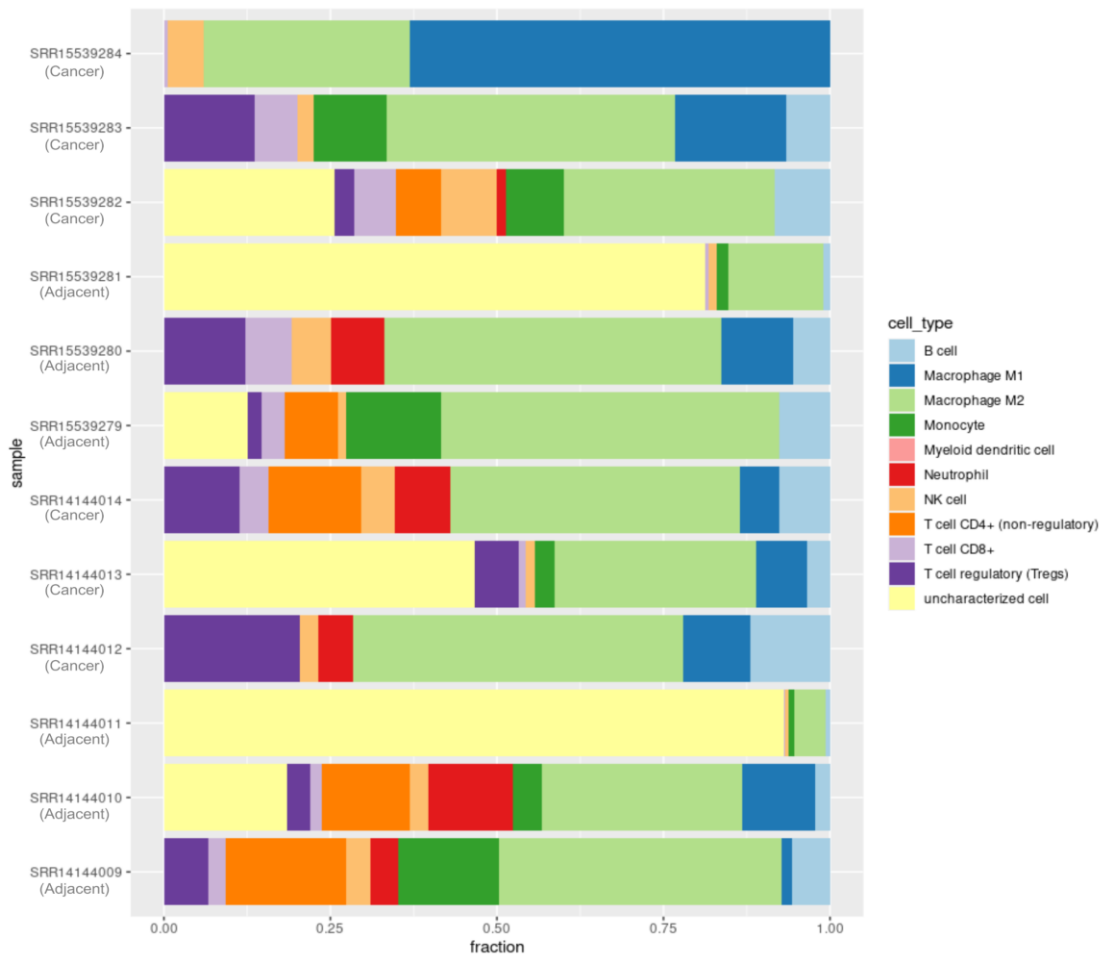


**Fig. 8.** The bar chart depicts scores for cell-type fractions using quanTIseq.

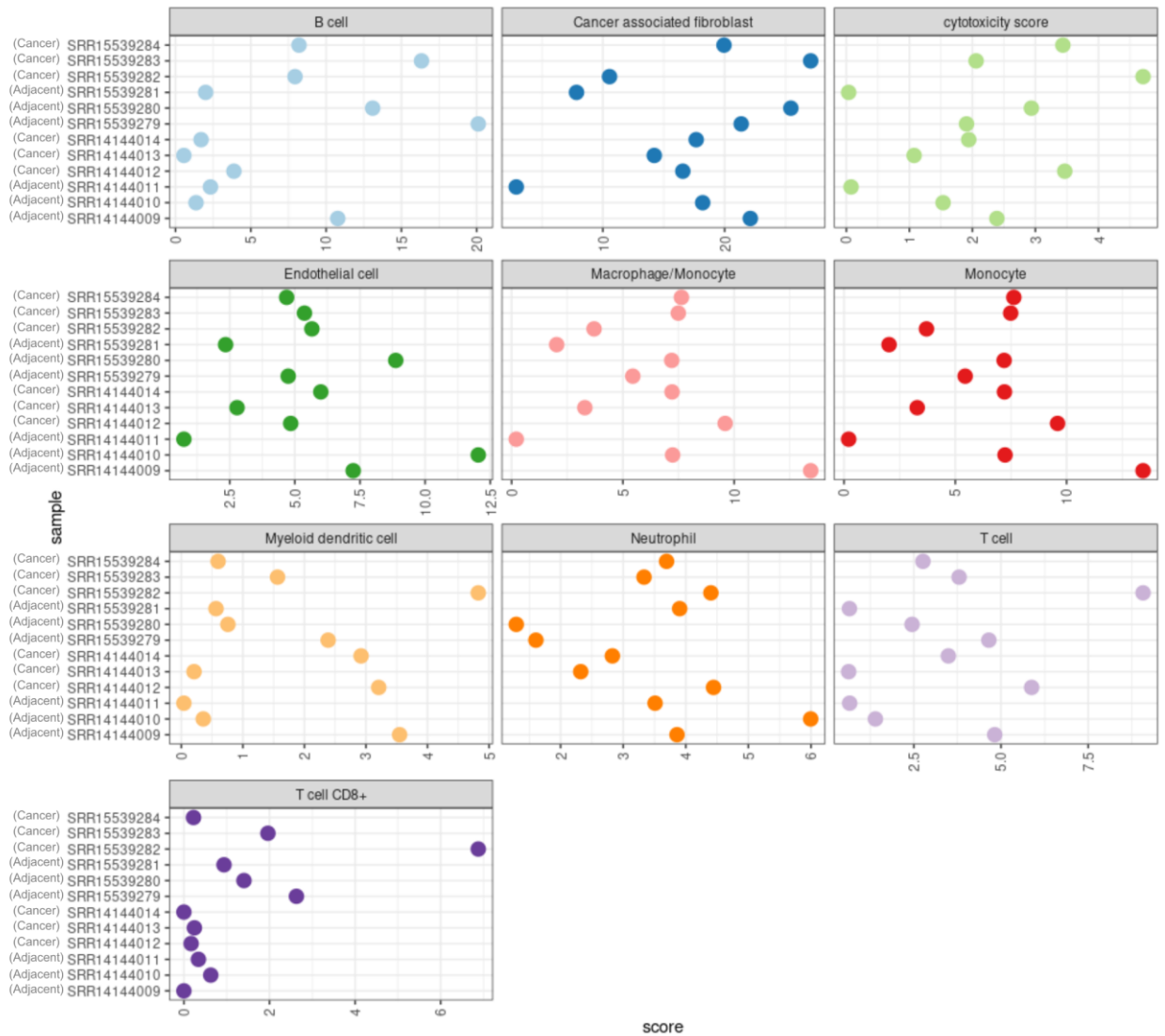


**Fig. 9.** The dot plot depicts scores per cell-type fractions using MCPcounter.

## DISCUSSION

Pancreatic cancer stands as a highly lethal disease, marked by an escalating incidence and dismal prognosis. The GLOBOCAN 2020 Statistics report reveals 495,773 reported cases and 466,003 fatalities globally, with a higher prevalence in men [3]. Various pancreatic cancer types, including endocrine, ductal, and exocrine, have been identified, with pancreatic ductal carcinoma in the exocrine region emerging as the most aggressive, representing 90 % of all cases and exhibiting poor prognosis [7, 8]. The aggressiveness of pancreatic ductal carcinoma has been linked to immune system dysregulation, characterized by insufficient immune activation and low immunogenicity. Additionally, alternative splicing, a post-transcriptional phenomenon, has been implicated in adverse effects on immune cell infiltration, contributing to immune system dysregulation [19, 20]. Unraveling alternative splicing mechanisms in immune system-related dysregulated genes is crucial for understanding the progression and development of PDAC.

The identified common immune-infiltrating genes (EPHA2, GNG11, CRHBP, and FCER1A) in both datasets (GSE171485 and GSE119794) might be involved in the proliferation and poor prognosis of PDAC. The upregulated gene EPHA2, a receptor tyrosine kinase, is involved in cell proliferation regulation, and cell-cell adhesion. Its frequent overexpression in PDAC has been linked to immune evasive characteristics [39–41]. However, the downregulated genes (GNG11, CRHBP, and FCER1A) need further investigation. GNG11, involved in the transmembrane

signaling system, is a member of the G protein  $\gamma$  family and lacks comprehensive exploration in PDAC, warranting further study [42]. CRHBP (corticotrophin-releasing hormone binding protein gene) and FCER1A ( $\alpha$ -subunit of the high-affinity immunoglobulin E receptor) are also underexplored in PDAC, and their potential roles in immune response dysregulation and molecular functions necessitate more attention for a better prognosis [43, 44].

Moreover, immune infiltration-related genes are crucial for the biological functioning of immune infiltration into the tumor microenvironment (TME). Dysregulation in the expression of these genes is associated with tumor development and progression [45]. Analyzing the expression of immune-related genes in the TME is essential for developing effective immunotherapeutic strategies against PDAC.

The functional enrichment analysis, particularly the Gene Ontology Molecular Function (GO MF) analysis, elucidated the dysregulated molecular functions of the upregulated and downregulated immune-related genes. The upregulated gene EPHA2 exhibited dysregulated molecular functions such as transmembrane receptor protein kinase activity, transmembrane receptor protein tyrosine kinase activity, protein tyrosine kinase activity, and cadherin binding. These molecular functions, when overexpressed, promote increased cell adhesion, ensure tissue integrity, favor collective cell migration, and modulate intracellular signaling. Moreover, they exert immunomodulatory effects on immune cells, recruiting them to the tumor microenvironment (TME). The upregulation of these molecular functions, resulting from the production of non-functional isoforms due to cancer, may lead to immune suppression [46, 47].

Conversely, downregulated genes suppressed the molecular functions of tumor cells, primarily encompassing GTPase activity and ribonucleoside triphosphate phosphatase activity. The downregulation of these molecular functions in cancer induces tumorigenesis through increased cell proliferation and differentiation. It also contributes to the dysregulation of immune cells such as macrophages, phagocytes, monocytes, natural killer cells, and lymphocytes [48]. Hence, the dysregulation of immune infiltration genes suggests an estimation of immune cell fractions in the tumor microenvironment.

The cancer microenvironment plays a crucial role in cancer treatment, particularly immunotherapy, providing insights into non-cancerous cells present in the tumor, especially immune cells. The analysis from quanTIseq (deconvolution-based) and MCPcounter (Marker-gene-based) methods demonstrated that almost all immune cell types are abundantly present in cancer samples. B cells, macrophages, natural killer cells, cytotoxicity scores, T-cells, endothelial cells, monocytes, and neutrophils were found in significant levels in cancer cells. B cells and T cells have well-known roles in anti-cancer immunity, with B cells also linked to pro-tumorigenic potential [49]. Natural killer cells exhibit tumor-antagonizing immune activities, promoting anti-tumor responses. However, the presence of macrophages in the tumor microenvironment has been associated with immunosuppression and tumor progression [50]. Endothelial cells contribute to tumor angiogenesis, act as a major source of cancer-associated fibroblasts, and play a role in mediating immune responses in the tumor microenvironment [51]. Cancer-associated fibroblasts are known for promoting tumor progression and are considered promising targets for the treatment of various cancers [52]. CD8<sup>+</sup> T-cells, major drivers of immunity against cancer, were observed in large amounts in cancer samples, while T cell regulatory (Tregs), associated with both tumor progression and anti-tumor immunity, were also present in considerable amounts. Tregs are linked to immune escape mechanisms in tumors [53, 54].

Isoform switching (AS) is a complex and highly regulated process that contributes to proteome diversity. In normal cells, isoforms play a crucial role in regulating various biological processes; however, their abnormal expression contributes to tumorigenesis [55]. There are five major types of alternative splicing events regarding splice site selection, including (exon skipping, mutually exclusive exons, intron retention, alternative 5 splice site, and alternative 3 splice site) [56]. In mammals, intron retention events are more enriched than exon-skipping mechanisms. However, in cancer cells, exon skipping events are frequently observed, with a

30% higher rate than in normal cells [55]. Isoform switching leads to the loss of DNA sequences encoding protein domains, significant changes in amino acid sequences, alteration of protein domains, and modification of signal peptides. These changes in domain structure through isoform switching can result in dysregulated signal transduction and protein-protein interactions [57]. Moreover, the production of noncanonical and cancer-specific mRNA transcripts due to aberrant alternative splicing can lead to the loss of function in tumor suppressors or activation of oncogenes, contributing to the progression of cancer pathways and malignancies [58]. Dysregulation in alternative splicing events is associated with various cellular dysfunctions, including tumorigenesis, immunological diseases, and infectious diseases. Isoform switching in immune-related genes can dysregulate the immune system, showing adverse effects on immune cell infiltration.

Isoforms with increased usage in PDAC were identified from the upregulated gene *EPHA2* and downregulated genes (*GNG11*, *CRHBP*, and *FCER1A*). For the upregulated gene *EPHA2*, a novel nonsense-mediated decay (NMD) isoform (MSTRG.377.2) was predicted to have increased usage in cancer. In the case of downregulated gene *FCER1A*, the isoform switching analysis revealed that a non-coding isoform (ENST00000693622) with intronic retention had significant usage in patients. *FCER1A*, encoding Fc Epsilon Receptor Ia, is a protein-coding receptor gene responsible for inducing allergic reactions in response to allergens and secreting cytokines [59].

While previous studies by Wu et al. [60] and Lin et al. [61] did not specifically focus on investigating immune infiltrating genes, emphasizing the exploration of novel dysregulated genes in PDAC versus normal tissues as potential therapeutic targets, this study utilized bulk RNA datasets to explore particularly novel immune-infiltrating genes as potential therapeutic targets for PDAC.

In conclusion, this study unveiled significantly dysregulated immune biomarkers involved in the deregulation of key immunological and normal cellular processes, ultimately contributing to PDAC. Four novel immune dysregulated genes (*EPHA2*, *CRHBP*, *GNG11*, and *FCER1A*) were identified as significantly dysregulated in PDAC. Additionally, isoform switching and immune response analysis of immune system-related dysregulated genes revealed dysregulation of the immune system and immune cell infiltration at the tumor site, potentially contributing to the development and progression of PDAC. The study also highlighted that several immune genes and their responses are hindered due to the production of multiple non-functional or pathogenic isoforms. Further studies on these isoforms and their effects on protein function are proposed. These immune biomarkers hold potential significance in therapeutics and the exploration of novel diagnostic possibilities. However, robust experimental validation is essential to confirm the *in silico* findings and outcomes of this study.

## CONCLUSIONS

PDAC is a highly lethal and aggressive malignancy, with a global prevalence rate of 49.8 per million and a mortality rate of 57.7 per million. The RNA-seq analysis of two datasets (GSE171485 and GSE119794) revealed a total of 484 differentially expressed genes (351 upregulated and 133 downregulated) in the GSE171485 dataset. In the GSE119794 dataset, a total of 517 significantly dysregulated genes were identified, with 249 genes upregulated and 268 genes downregulated. Specifically, four immune-related genes (*EPHA2*, *CRHBP*, *GNG11*, and *FCER1A*) were identified as novel immune-infiltrating genes not previously reported in PDAC, particularly in the context of alternative splicing leading to isoform switching. The prediction of immune cell infiltration in pancreatic cancer uncovered dysregulated immune responses due to the formation of pathogenic isoforms. Gene Ontology (GO) molecular function analysis of differentially expressed common immune genes among both datasets revealed dysregulated molecular functions, including protein binding, IgE binding, CXCR chemokine receptor binding, ephrin receptor activity, cobalamin binding, and chemokine activity. The

downregulation of these functions in cancer suggests induction of tumorigenesis through increased cell proliferation and dysregulation of immune cells. The study uncovered the potentially significant role of the immune system in the development and progression of PDAC. However, the impact of the identified isoform biomarkers on treating PDAC remains unclear without future investigations and experimental validations. The study proposes further investigations to explore the functional aspects of pathogenic and non-functional isoforms. The proposed immune biomarkers are suggested for use in the development of efficient immunotherapeutic treatments against PDAC.

## REFERENCES

1. Zhang L., Sanagapalli S., Stoita A. Challenges in diagnosis of pancreatic cancer. *World J. Gastroenterol.* 2018. V. 24. No. 19. P. 2047–2060.
2. Rawla P., Sunkara T., Gaduputi V. Epidemiology of Pancreatic Cancer: Global Trends, Etiology and Risk Factors. *World J. Oncol.* 2019. V. 10. No. 1. P. 10–27.
3. Sung H., Ferlay J., Siegel R.L., Laversanne M., Soerjomataram I., Jemal A., Bray F. Global Cancer Statistics 2020: GLOBOCAN Estimates of Incidence and Mortality Worldwide for 36 Cancers in 185 Countries. *CA Cancer J. Clin.* 2021. V. 71. No. 3. P. 209–249.
4. Fukushima N., Zamboni G. Histologic Classification and Staging of Cystic Neoplasms. In: *The Pancreas: An Integrated Textbook of Basic Science, Medicine, and Surgery*, Third Edition.. John Wiley & Sons, Ltd, 2018. P. 573–579. doi: [10.1002/9781119188421.ch74](https://doi.org/10.1002/9781119188421.ch74)
5. Diab M., Philip P.A. Uncommon Cancers of the Pancreas. In: *Textbook of Uncommon Cancer*. John Wiley & Sons, Ltd, 2017. P. 429–443. doi: [10.1002/9781119196235.ch29](https://doi.org/10.1002/9781119196235.ch29)
6. Rawla P., Sunkara T., Gaduputi V. Epidemiology of Pancreatic Cancer: Global Trends, Etiology and Risk Factors. *World J. Oncol.* 2019. V. 10. No. 1. P. 10–27.
7. Collisson E.A., Bailey P., Chang D.K., Biankin A.V. Molecular subtypes of pancreatic cancer. *Nat. Rev. Gastroenterol. Hepatol.* 2019. V. 16. No. 4. P. 207–220.
8. Gao H.L., Wang W.Q., Yu X.J., Liu L. Molecular drivers and cells of origin in pancreatic ductal adenocarcinoma and pancreatic neuroendocrine carcinoma. *Exp. Hematol. Oncol.* 2020. V. 22. No. 9. P. 28.
9. Mostafa M.E., Erbarut-Seven I., Pehlivanoglu B., Adsay V. Pathologic classification of “pancreatic cancers”: current concepts and challenges. *Chin. Clin. Oncol.* 2018. V. 6. No. 6. P. 59–59.
10. Oldfield L.E., Connor A.A., Gallinger S. Molecular Events in the Natural History of Pancreatic Cancer. *Trends Cancer.* 2017. V. 1. V. 3. No. 5. P. 336–346.
11. Grimont A., Leach S.D., Chandwani R. Uncertain Beginnings: Acinar and Ductal Cell Plasticity in the Development of Pancreatic Cancer. *Cell. Mol. Gastroenterol. Hepatol.* 2022 Jan 1;13(2):369–382.
12. Deshwar A.B., Sugar E., Torto D., Jesus-Acosta A.D., Weiss M.J., Wolfgang C.L, Le D., He J., Burkhart R., Zheng L. et al. Diagnostic intervals and pancreatic ductal adenocarcinoma (PDAC) resectability: a single-center retrospective analysis. *Ann. Pancreat. Cancer.* 2018. V. 1. No. 2.
13. Moffat G.T., Epstein A.S., O’Reilly E.M. Pancreatic cancer – A disease in need: Optimizing and integrating supportive care. *Cancer.* 2019. V. 125. No. 22. P. 3927–3935.
14. Sahin I.H., Askan G., Hu Z.I., O’Reilly E.M. Immunotherapy in pancreatic ductal adenocarcinoma: an emerging entity? *Ann. Oncol.* 2017. V. 28. No. 12. P. 2950–61.
15. Karamitopoulou E. Tumour microenvironment of pancreatic cancer: immune landscape is dictated by molecular and histopathological features. *Br. J. Cancer.* 2019. V. 121. No. 1. P. 5–14.
16. Riquelme E., Maitra A., McAllister F. Immunotherapy for Pancreatic Cancer: More than Just a Gut Feeling. *Cancer Discov.* 2018. V. 8. No. 4. P. 386–388.

17. Lu J., Wei S., Lou J., Yin S., Zhou L., Zhang W., Zheng S. Systematic Analysis of Alternative Splicing Landscape in Pancreatic Adenocarcinoma Reveals Regulatory Network Associated with Tumorigenesis and Immune Response. *Med. Sci. Monit.* 2020. V. 26. doi: [10.12659/MSM.925733](https://doi.org/10.12659/MSM.925733)
18. Zhang Y., Velez-Delgado A., Mathew E., Li D., Mendez F.M., Flannagan K., Rhim A.D., Simeone D.M., Beatty G.L., di Magliano M.P. Myeloid cells are required for PD-1/PD-L1 checkpoint activation and the establishment of an immunosuppressive environment in pancreatic cancer. *Gut.* 2017. V. 66. No. 1. P. 124–136. doi: [10.1136/gutjnl-2016-312078](https://doi.org/10.1136/gutjnl-2016-312078)
19. Chen B., Deng T., Deng L., Yu H., He B., Chen K., Zheng C., Wang D., Wang Y., Chen G. Identification of tumour immune microenvironment-related alternative splicing events for the prognostication of pancreatic adenocarcinoma. *BMC Cancer.* 2021. V. 21. No. 1. P. 1211.
20. Marzese D.M., Manughian-Peter A.O., Orozco J.I.J., Hoon D.S.B. Alternative splicing and cancer metastasis: prognostic and therapeutic applications. *Clin. Exp. Metastasis.* 2018. V. 35. No. 5. P. 393–402.
21. Kawalerski R.R., Leach S.D., Escobar-Hoyos L.F. Pancreatic cancer driver mutations are targetable through distant alternative RNA splicing dependencies. *Oncotarget.* 2021. V. 12. No. 6. P. 525–533.
22. Venkat S., Alahmari A.A., Feigin M.E. Drivers of Gene Expression Dysregulation in Pancreatic Cancer. *Trends Cancer.* 2021. V. 7. No. 7. P. 594–605.
23. Barrett T., Wilhite S.E., Ledoux P., Evangelista C., Kim I.F., Tomashevsky M., Marshall K.A., Phillippy K.H., Sherman P.M., Holko M., et al. NCBI GEO: archive for functional genomics data sets – update. *Nucleic Acids Res.* 2013. V. 41. No. D1. P. D991–D995. doi: [10.1093/nar/gks1193](https://doi.org/10.1093/nar/gks1193)
24. Barrett T., Troup D.B., Wilhite S.E., Ledoux P., Rudnev D., Evangelista C., Kim I.F., Soboleva A., Tomashevsky M., Marshall K.A., et al. NCBI GEO: archive for high-throughput functional genomic data. *Nucleic Acids Res.* 2009. V. 37. No. suppl\_1. P. D885–D890. doi: [10.1093/nar/gkn764](https://doi.org/10.1093/nar/gkn764)
25. Brown J., Pirrung M., McCue L.A. FQC Dashboard: integrates FastQC results into a web-based, interactive, and extensible FASTQ quality control tool. *Bioinformatics.* 2017. V. 33. No. 19. P. 3137–3139.
26. Chen S., Zhou Y., Chen Y., Gu J. fastp: an ultra-fast all-in-one FASTQ preprocessor. *Bioinformatics.* 2018. V. 34. No. 17. P. i884–i890.
27. Tarasov A., Vilella A.J., Cuppen E., Nijman I.J., Prins P. Sambamba: fast processing of NGS alignment formats. *Bioinformatics.* 2015. V. 31. No. 12. P. 2032–4.
28. Pertea M., Pertea G.M., Antonescu C.M., Chang T.C., Mendell J.T., Salzberg S.L. StringTie enables improved reconstruction of a transcriptome from RNA-seq reads. *Nat. Biotechnol.* 2015. V. 33. No. 3. P. 290–5.
29. Papatheodorou I., Moreno P., Manning J., Fuentes A.M.P., George N., Fexova S., Fonseca N.A., Füllgrabe A., Green M., Huang N., et al. Expression Atlas update: from tissues to single cells. *Nucleic Acids Res.* 2020. V. 48. No. D1. P. D77–83.
30. Tang Z., Kang B., Li C., Chen T., Zhang Z. GEPIA2: an enhanced web server for large-scale expression profiling and interactive analysis. *Nucleic Acids Res.* 2019. V. 47. No. W1. P. W556–60.
31. Xie Z., Bailey A., Kuleshov M.V., Clarke D.J.B., Evangelista J.E., Jenkins S.L., Lachmann A., Wojciechowicz M.L., Kropiwnicki E., Jagodnik K.M., Jeon M., Ma'ayan A. Gene Set Knowledge Discovery with Enrichr. *Curr. Protoc.* 2021. V. 1. No. 3. P. e90. doi: [10.1002/cpz1.90](https://doi.org/10.1002/cpz1.90)
32. Ianevski A., Giri A.K., Aittokallio T. Fully-automated and ultra-fast cell-type identification using specific marker combinations from single-cell transcriptomic data. *Nat. Commun.* 2022. V. 13. No. 1. P. 1246.

33. Garcia-Moreno A., López-Domínguez R., Villatoro-García J.A., Ramirez-Mena A., Aparicio-Puerta E., Hackenberg M., Pascual-Montano A., Carmona-Saez P. Functional Enrichment Analysis of Regulatory Elements. *Biomedicines*. 2022. V. 10. No. 3. P. 590. doi: [10.3390/biomedicines10030590](https://doi.org/10.3390/biomedicines10030590)
34. Chen L., Chen K., Hong Y., Xing L., Zhang J., Zhang K., Zhang Z. The landscape of isoform switches in sepsis: a multicenter cohort study. *Sci. Rep.* 2022. V. 12. No. 1. P. 10276. doi: [10.1038/s41598-022-14231-9](https://doi.org/10.1038/s41598-022-14231-9)
35. Finotello F., Mayer C., Plattner C., Laschober G., Rieder D., Hackl H., Krogsdam A., Loncova Z., Posch W., Wilflingseder D. et al. Molecular and pharmacological modulators of the tumor immune contexture revealed by deconvolution of RNA-seq data. *bioRxiv*. 2018. doi: [10.1101/223180](https://doi.org/10.1101/223180)
36. Huang S., Song Z., Zhang T., He X., Huang K., Zhang Q., Shen J., Pan J. Identification of Immune Cell Infiltration and Immune-Related Genes in the Tumor Microenvironment of Glioblastomas. *Front. Immunol.* 2020. V. 11. doi: [10.3389/fimmu.2020.585034](https://doi.org/10.3389/fimmu.2020.585034)
37. Sturm G., Finotello F., List M. Immunedeconv: An R Package for Unified Access to Computational Methods for Estimating Immune Cell Fractions from Bulk RNA-Sequencing Data. In: *Bioinformatics for Cancer Immunotherapy. Methods in Molecular Biology*, vol 2120. Ed. Boegel S. New York, NY: Springer US; 2020. P. 223–332. doi: [10.1007/978-1-0716-0327-7\\_16](https://doi.org/10.1007/978-1-0716-0327-7_16)
38. Becht E., Giraldo N.A., Lacroix L., Buttard B., Elarouci N., Petitprez F., Selves J., Laurent-Puig P., Sautès-Fridman C., Fridman W.H., de Reyniès A. Estimating the population abundance of tissue-infiltrating immune and stromal cell populations using gene expression. *Genome Biol.* 2016. V. 17. No. 1. P. 218.
39. Le Large T.Y.S., Mantini G., Meijer L.L., Pham T.V., Funel N., van Grieken N.C.T., Kok B., Knol J., van Laarhoven H.W.M., Piersma S.R., et al. Microdissected pancreatic cancer proteomes reveal tumor heterogeneity and therapeutic targets. *JCI Insight*. 2020. V. 5. No. 15. P. e138290.
40. Hill W., Zaragkoulias A., Salvador-Barbero B., Parfitt G.J., Alatsatianos M., Padilha A., Porazinski S., Woolley T.E., Morton J.P., Sansom O.J., Hogan C. EPHA2-dependent outcompetition of KRASG12D mutant cells by wild-type neighbors in the adult pancreas. *Curr. Biol.* 2021. V. 31. No. 12. P. 2550–2560.e5. doi: [10.1016/j.cub.2021.03.094](https://doi.org/10.1016/j.cub.2021.03.094)
41. Iizumi M., Hosokawa M., Takehara A., Chung S., Nakamura T., Katagiri T., Eguchi H., Ohigashi H., Ishikawa O., Nakamura Y., Nakagawa H. EphA4 receptor, overexpressed in pancreatic ductal adenocarcinoma, promotes cancer cell growth. *Cancer Sci.* 2006. V. 97. No. 11. P. 1211–1216. doi: [10.1111/j.1349-7006.2006.00313.x](https://doi.org/10.1111/j.1349-7006.2006.00313.x)
42. Haouas H., Haouas S., Uzan G., Hafsia A. Identification of new markers discriminating between myeloid and lymphoid acute leukemia. *Hematology*. 2010. V. 15. No. 4. P. 193–203.
43. Iovanna J., Dusetti N. Speeding towards individualized treatment for pancreatic cancer by taking an alternative road. *Cancer Lett.* 2017. V. 410. P. 63–67.
44. Luo Y. The characteristic of stem-related genes with pancreatic carcinoma cell after irradiation. *Heliyon*. 2023. V. 9. No. 6. P. e17074.
45. Yang H., Zhao L., Zhang Y., Li F.F. A comprehensive analysis of immune infiltration in the tumor microenvironment of osteosarcoma. *Cancer Med.* 2021. V. 10. No. 16. P. 5696–5711.
46. Zalpoor H., Aziziyan F., Liaghat M., Bakhtiyari M., Akbari A., Nabi-Afjadi M., Forghaniesfidvajani R., Rezaei N. The roles of metabolic profiles and intracellular signaling pathways of tumor microenvironment cells in angiogenesis of solid tumors. *Cell Commun. Signal.* 2022. V. 20. No. 1. P. 186.
47. Sommariva M., Gagliano N. E-Cadherin in Pancreatic Ductal Adenocarcinoma: A Multifaceted Actor during EMT. *Cells*. 2020. V. 9. No. 4. P. 1040.
48. Li H., Wu M., Zhao X. Role of chemokine systems in cancer and inflammatory diseases.

- MedComm*. 2022. V. 3. No. 2. P. e147.
49. Tan R., Nie M., Long W. The role of B cells in cancer development. *Front. Oncol.* 2022. V. 12. No. 958756. doi: [10.3389/fonc.2022.958756](https://doi.org/10.3389/fonc.2022.958756)
  50. Dong Y., Wan Z., Gao X., Yang G., Liu L. Reprogramming Immune Cells for Enhanced Cancer Immunotherapy: Targets and Strategies. *Front. Immunol.* 2021. V. 12 No. 609762. doi: [10.3389/fimmu.2021.609762](https://doi.org/10.3389/fimmu.2021.609762)
  51. Nagl L., Horvath L., Pircher A., Wolf D. Tumor Endothelial Cells (TECs) as Potential Immune Directors of the Tumor Microenvironment – New Findings and Future Perspectives. *Front. Cell Dev. Biol.* 2020. V. 8. P. 766. doi: [10.3389/fcell.2020.00766](https://doi.org/10.3389/fcell.2020.00766)
  52. Luo N. Editorial: Tumor microenvironment in cancer hallmarks and therapeutics. *Front. Mol. Biosci.* 2022. V. 9. P. 1019830. doi: [10.3389/fmolb.2022.1019830](https://doi.org/10.3389/fmolb.2022.1019830)
  53. van der Leun A.M., Thommen D.S., Schumacher T.N. CD8+ T cell states in human cancer: insights from single-cell analysis. *Nat. Rev. Cancer.* 2020. V. 20. P. 218–232. doi: [10.1038/s41568-019-0235-4](https://doi.org/10.1038/s41568-019-0235-4)
  54. Li C., Jiang P., Wei S., Xu X., Wang J. Regulatory T cells in tumor microenvironment: new mechanisms, potential therapeutic strategies and future prospects. *Mol. Cancer.* 2020. V. 19. No. 1. P. 116.
  55. Karakulak T., Moch H., von Mering C., Kahraman A. Probing Isoform Switching Events in Various Cancer Types: Lessons From Pan-Cancer Studies. *Front. Mol. Biosci.* 2021. V. 8. Article No. 726902. doi: [10.3389/fmolb.2021.726902](https://doi.org/10.3389/fmolb.2021.726902)
  56. Zhang Y., Weh K.M., Howard C.L., Riethoven J.J., Clarke J.L., Lagisetty K.H., Lin J., Reddy R.M., Chang A.C., Beer D.G. et al. Characterizing isoform switching events in esophageal adenocarcinoma. *Mol. Ther – Nucleic Acids.* 2022. V. 29. P. 749–768. doi: [10.1016/j.omtn.2022.08.018](https://doi.org/10.1016/j.omtn.2022.08.018)
  57. Vitting-Seerup K., Sandelin A. The Landscape of Isoform Switches in Human Cancers. *Mol. Cancer Res.* 2017. V. 15. No. 9. P. 1206–1220.
  58. Chen J., Weiss W.A. Alternative splicing in cancer: implications for biology and therapy. *Oncogene.* 2015. V. 34. No. 1. P. 1–14.
  59. Potaczek D.P., Przytulska-Szczerbik A., Bazan-Socha S., Nastalek M., Wojas-Pelc A., Okumura K., Nishiyama C., Jurczynszyn A., Undas A., Wypasek E. Interaction between functional polymorphisms in FCER1A and TLR2 and the severity of atopic dermatitis. *Hum Immunol.* 2020. V. 81. No. 12. P. 709–713. doi: [10.1016/j.humimm.2020.08.002](https://doi.org/10.1016/j.humimm.2020.08.002)
  60. Wu H., Tian W., Tai X., Li X., Li Z., Shui J., Yu J., Wang Z., Zhu X. Identification and functional analysis of novel oncogene DDX60L in pancreatic ductal adenocarcinoma. *BMC Genomics.* 2021. V. 22. No. 1. P. 833.
  61. Lin J., Wu Y.J., Liang X., Ji M., Ying H.M., Wang X.Y., Sun X., Shao C.H., Zhan L.X., Zhang Y. Network-based integration of mRNA and miRNA profiles reveals new target genes involved in pancreatic cancer. *Mol. Carcinog.* 2019. V. 58. No. 2. P. 206–218. doi: [10.1002/mc.22920](https://doi.org/10.1002/mc.22920)

Received 29.11.2023.

Revised 04.01.2024.

Published 27.02.2024.